UNIVERSITI PUTRA MALAYSIA

OPTIMIZATION OF ENERGY WINDOW FOR DIFFERENT BODY MASS INDEX IN BIOGRAPH TRUEPOINT POSITRON EMISSION TOMOGRAPHY IMAGING SYSTEM

MARIANIE BINTI MUSARUDIN

FK 2015 95

OPTIMIZATION OF ENERGY WINDOW FOR DIFFERENT BODY MASS INDEX IN BIOGRAPH TRUEPOINT POSITRON EMISSION TOMOGRAPHY IMAGING SYSTEM

By

MARIANIE BINTI MUSARUDIN

Thesis Submitted to the School of Graduate Studies, Universiti Putra Malaysia, in Fulfillment of the Requirements for the Degree of Doctor of Philosophy

June 2015

DEDICATIONS

In dedication to my beloved parents,

my best companion in life, Ab. Rashid Jusoh and

our children, Soffiya Zahra and Muhammad Al Fateh ♡

Abstract of thesis presented to the Senate of Universiti Putra Malaysia in fulfillment of the requirement for the degree of Doctor of Philosophy

OPTIMIZATION OF ENERGY WINDOW FOR DIFFERENT BODY MASS INDEX IN BIOGRAPH TRUEPOINT POSITRON EMISSION TOMOGRAPHY IMAGING SYSTEM

By

MARIANIE BINTI MUSARUDIN

June 2015

Chair: M. Iqbal Bin Saripan, Ph.D.
Faculty: Engineering

Internal scattering in patient's body is one of the key factors that leads to PET image quality degradation. This interaction affects the imaging performance in the sense of mispositioning of the annihilation position and coincidence data lost. One of the factors that determines the probability of this interaction is the patient's body weight. In practice, the impact of scattering is worse with the increment of the patient's body weight. Thus, optimization of scatter events contribution in the raw data prior to image reconstruction is vital as it determines the quality of PET image generated. The quality of the image, which eventually help to determine the tumor detection rate, will improve the survival rate of the cancer patient.

Various methods were proposed and identified by the previous studies to minimize the contribution of both patient and detector's scatter to the raw data. This study, was nonetheless achieved the above target through the analysis of signal processing. The aim of this study is to define the optimal energy threshold level for the different groups of patient's body. The definition was done based on the phantom's modeling. Various patient's sizes in the range of 44.0 kg to 99.0 kg which yield diameters of 20 cm to 30 cm were modeled using Monte Carlo N-Particle code version 5 (MCNP5). The impact of phantom's masses to the several measurement parameters like scatter fraction, tumor visibility and signal to noise ratio (SNR) also was tested in order to define the optimal energy threshold level for each phantom size. Various energy threshold levels were implemented on the simulated data.

Evaluation of tumor SNR on the reconstructed image was the core measure used in this study. The optimal energy threshold value was defined when the maximum SNR was

yielded at the respective energy window used. At the end of this study, we managed to propose an optimal energy window for the underweight, normal and obese patient. The obese phantom which lost more photons via photon scattering and attenuation thus required up to 20.00% and 27.27% larger energy window than the underweight and normal phantom respectively. These threshold values, which are 2.30% to 13.79% varies from the default energy window that commonly practiced, improves the SNR up to 1.24%.

At the end of this study, we managed to propose an equation that gave correlations among the body weight, the tumor to background ratio (TBR) and the optimal energy threshold level. The derivation of this equation was done based on the data obtained in this study. The proposed equation, therefore allows definition of the optimal energy window for any condition of imaging, particularly those related to the weight of the patient's body and TBR or standard uptake values (SUV) of the tumor.

ii

Abstrak tesis yang dikemukakan kepada Senat Universiti Putra Malaysia sebagai memenuhi keperluan untuk ijazah Doktor Falsafah.

PENGOPTIMUMAN TETINGKAP TENAGA UNTUK INDEKS JISIM BADAN YANG BERBEZA DALAM SISTEM PENGIMEJAN TOMOGRAFI PANCARAN POSITRON BIOGRAPH TRUEPOINT

Oleh

MARIANIE BINTI MUSARUDIN

Jun 2015

Pengerusi: M. Iqbal Bin Saripan, Ph.D.
Fakulti: Kejuruteraan

Serakan di dalam badan pesakit adalah salah satu faktor utama yang membawa kepada kemerosotan kualiti imej PET. Interaksi ini memberi kesan kepada prestasi pengimejan dari segi kesalahan posisi penghapusan dan kehilangan data kesekenaan. Salah satu faktor yang menentukan kebarangkalian interaksi ini adalah berat badan pesakit. Dalam praktikal, impak serakan pesakit bertambah buruk dengan peningkatan berat badan pesakit. Oleh itu, pengoptimuman sumbangan data serakan dalam data mentah sebelum pembinaan semula imej adalah penting kerana ia menentukan kualiti imej PET yang dihasilkan. Kualiti imej, yang akhirnya membantu menentukan kadar pengesanan tumor, akan meningkatkan kadar kelangsungan hidup pesakit kanser.

Pelbagai kaedah telah dicadangkan dan dikenalpasti oleh kajian-kajian sebelum ini untuk meminimakan sumbangan kedua-dua serakan pesakit dan pengesan terhadap data. Kajian ini walaubagaimanapun dilaksanakan melalui analisa pemprosesan isyarat. Matlamat kajian ini adalah untuk mendefinisikan had tenaga optimum untuk kumpulan badan manusia yang berbeza. Definisi ini adalah berdasarkan kepada permodelan fantom. Pelbagai saiz pesakit dalam lingkungan 44.0 kg hingga 99.0 kg yang menghasilkan diameter fantom 20 cm hingga 30 cm telah dimodelkan dengan menggunakan kod Monte Carlo N-Particle versi ke-5 (MCNP5). Kesan jisim fantom terhadap beberapa parameter pengukuran seperti pecahan serakan, kebolehlihatan ketumbuhan dan nisbah hingar kepada isyarat (SNR) telah diuji untuk mendefinisikan tahap had tenaga yang optimum untuk setiap saiz fantom. Pelbagai peringkat had tenaga telah dilaksanakan kepada data simulasi.

Penilaian SNR ketumbuhan pada imej yang dibina semula adalah langkah utama yang digunakan dalam kajian ini. Nilai had tenaga yang optimum ditakrifkan apabila SNR yang maksimum dihasilkan pada tetingkap tenaga yang digunakan. Di akhir kajian ini,

iii

kami berjaya mencadangkan tetingkap tenaga optimum bagi pesakit yang kekurangan berat badan, normal dan obes. Fantom obes yang kehilangan lebih banyak foton melalui penyerakan foton dan pengecilan foton maka memerlukan tetingkap tenaga yang sehingga 20.00% dan 27.27% lebih besar berbanding fantom yang masing-masing kekurangan berat badan dan normal. Nilai-nilai ambang ini, yang 2.30% hingga 13.79% berbeza daripada tetingkap tenaga tetap yang biasa dipraktikkan, meningkatkan SNR sehingga 1.24%.

Di akhir kajian ini, kami berjaya mencadangkan satu persamaan yang menghubung kaitkan antara berat badan, nisbah tumor kepada latar belakang (TBR) dan nilai had tenaga yang optimum. Penerbitan persamaan ini dilakukan berdasarkan kepada data yang diperolehi dalam kajian ini. Persamaan yang dicadangkan, dengan itu membolehkan tetingkap tenaga yang optimum didefinisikan untuk sebarang situasi pengimejan, terutamanya yang berkaitan dengan berat badan pesakit dan TBR atau nilai serapan piawai (SUV) tumor.

ACKNOWLEDGEMENTS

Mostly to God, the Compassionate the Merciful, through Him, all is possible.

The fulfillment of this program is indeed a challenging task which cannot be accomplished without the personal and practical support of numerous people. Thus, I would like to deeply thank the various people who provided me with useful and helpful assistance during my doctoral work. Without their invaluable and wise advice, this dissertation would not have reached to this stage.

I would especially like to thank my supervisor, Prof. Dr. M. Iqbal bin Saripan, for his warm encouragement and support. Throughout my doctoral research, his constant insight has helped my dissertation to mature. He has also helped me to develop independent thinking and to become a self-driven researcher. I am grateful to him for giving me his time and special attention.

I am also extremely grateful for receiving an exceptional assistance and coaching from my supervisory committee member, Prof. Dr. Abdul Jalil bin Nordin. He has invested much time to help me understand imaging more. I am also very thankful to Dr. Syamsiah binti Mashohor for her valuable guidance in image processing. The meetings with my supervisory committee members have continually stimulated my analytical thinking and greatly assisted me with data analysis and scientific writing.

I extend many thanks to my colleagues and friends, especially Dr. Wira Hidayat bin Mohd Saad for his invaluable time given to validate my research instruments. In fact, I feel a lot indebted to him not only for his teachings but also for the personal support that he has constantly offered me throughout my studies. Many thanks also to Ms Salasiah binti Mustafa and the team for their assistance during the data collection procedures.

Finally, I would like to thank my family. I indeed owe a lot to my husband Ab Rashid bin Jusoh for his incredible support and sacrifices that he has made throughout my candidature. Without his generous sacrifices, this accomplishment would have been impossible. I am especially indebted to my parents. Their encouragement, prayers, and teachings have always been with me.

Above all, I thank the Almighty for giving me my dear ones and granting me the opportunity to study in this university.

This thesis was submitted to the Senate of Universiti Putra Malaysia and has been accepted as fulfillment of the requirement for the degree of Doctor of Philosophy.

The members of the Supervisory Committee were as follows:

M. Iqbal Saripan, Ph.D.
Professor
Faculty of Engineering
Universiti Putra Malaysia
(Chairperson)

Abdul Jalil bin Nordin, M.D.
Professor
Faculty of Medicine and Health Science
Universiti Putra Malaysia
(Member)

Syamsiah Mashohor, Ph.D.
Senior Lecturer
Faculty of Engineering
Universiti Putra Malaysia
(Member)

_____
BUJANG KIM HUAT, Ph.D.
Professor and Dean
School of Graduate Studies
Universiti Putra Malaysia

Date:

TABLE OF CONTENTS

LIST OF TABLES

xiv

LIST OF FIGURES

LIST OF ABBREVIATIONS

1D	One-dimensional
2D	Two-dimensional
3D	Three-dimensional
^{18}F	Fluorine-18
μ	Attenuation Coefficient
BGO	Bismuth Germinate
BMI	Body Mass Index
CT	Computed Tomography
DOI	Depth-of-Interaction
EANM	European Association of Nuclear Medicine
FBP	Filtered back-projection
FDG	Fluorodeoxyglucose
FOV	Field of View
FWHM	Full Width Half Maximum
LOR	Line of Response
LSO	Lutetium Oxyorthosilicate
LySO	Lutetium Yttrium Orthosilicate
MCNP	Monte Carlo N-particle
MLEM	Maximum-Likelihood Expectation Maximization
MRI	Magnetic Resonance Imaging
MSE	Mean Square Error
NaI	Sodium Iodide
NECR	Noise Equivalent Count Rate
NEMA	National Electrical Manufacturers Association
OSEM	Ordered Subsets Expectation Maximization
PET	Positron Emission Tomography
PHA	Pulse Height Analyzer

PMT	Photomultiplier Tube
PTRAC	Particle Track Output Card
ROI	Region of interest
SNR	Signal-to-Noise Ratio
SPECT	Single Photon Emission Computed Tomography
SUV	Standard Uptake Values
TBR	Tumor to background ratio
TOF	Time-of-Flight

CHAPTER 1

INTRODUCTION

This chapter provides the introduction to the concerning issues of this research. The chapter is sub-sectioned into five sections: the background, problem statement, objectives, the scope and limitations of the research and research contribution.

1.1   The Background of the Study

For more than 10 decades, imaging technology has been used as an aiding tool in the clinical diagnosis, specifically in the areas of neurology and oncology. This technology has started since the discovery of X-rays by Wilhelm Conrad Roentgen in 1895 [1]. At first, the imaging technology focus was on the image formation by focusing X-rays through the patient's body. Since then, technological developments in medical imaging have continue to improve and grow. The two-dimensional (2D) X-ray imaging that provides a flat X-ray image thus limit the depth information and image contrast [2]. This limitation let to an introduction of Computed Tomography (CT) that offers three-dimensional (3D) cross-sectional image reconstruction from the 2D projection data [3]. In addition to the structural-based imaging, medical imaging is now moving towards functional-based imaging or also known as nuclear imaging. Today, functional-based imaging scanner like positron emission tomography (PET) and single photon emission computed tomography (SPECT) are widely practiced in clinical applications.

In this thesis, we concentrate on PET imaging with the detector material of interest of Lutetium Oxyorthosilicate (LSO). PET imaging is a nuclear medicine technique that produces images of body function began in 1950. Meanwhile, the first commercial positron imaging device was developed in 1980 [4]. At first, this device was specifically designed for the brain imaging. However, the high sensitivity of PET expands the application of this technology, particularly to the whole body imaging. The basis of photon detection in PET is principally similar to the other nuclear imaging technique like SPECT. The difference is PET works by detecting two coincidence photons that are emitted in opposite direction. PET radiotracer is initially injected into the patient's blood vessels. The decay and interaction processes within the patient's body, thus emits photons that are eventually detected by the scintillation detector. The PET image shows the distribution of the injected radiotracer within the patient's body as a function of the metabolic rate of each area. The higher metabolic rates of the tumor cells thus absorb more activity compared to the normal cells [5, 6].

The current morbidity and mortality rate of cancer in the world, particularly Malaysia makes such high sensitivity imaging tools needed in clinical practices. Several types of cancer are listed among the most reported causes of death, for instance, lung, breast and liver cancers in Malaysia. In 2003 to 2005, 116 per 100000 populations of cancer

1

incidence were reported in Peninsular Malaysia [7]. The value increased to 109.8 per 100000 populations in 2006 [8]. One of the reasons leading to the high cancer mortality rate is due to the late diagnosis of the disease. Therefore, early detection of the disease can increase the probability to cure the disease. This is in turn highly dependent on the performance of the imaging tools, specifically the quality of the reconstructed image. The high sensitivity PET imaging is now reported as the most accurate tool for cancer diagnosis and monitoring [9, 10]. Nevertheless, the performance of a PET imaging is influenced by multiple factors, that could be classified as physical, technical and biological factors [11–18].

The noisy nature of the PET image thus requires each single factor possible for the image quality enhancement to be considered. The processes of image processing start by the image acquisition, whereby the data are acquired either via one-dimensional (1D), 2D or 3D acquisition method. The step continues into the processing step that could be initialized by the pre-processing steps. Further post-processing steps are commonly implemented to enhance the quality of the image. The components of image processing are illustrated in Figure 1.1. The works present in this thesis are based on the technical aspect of the image acquisition, wherewith the optimal energy threshold level for different sizes of the patient's body was defined.
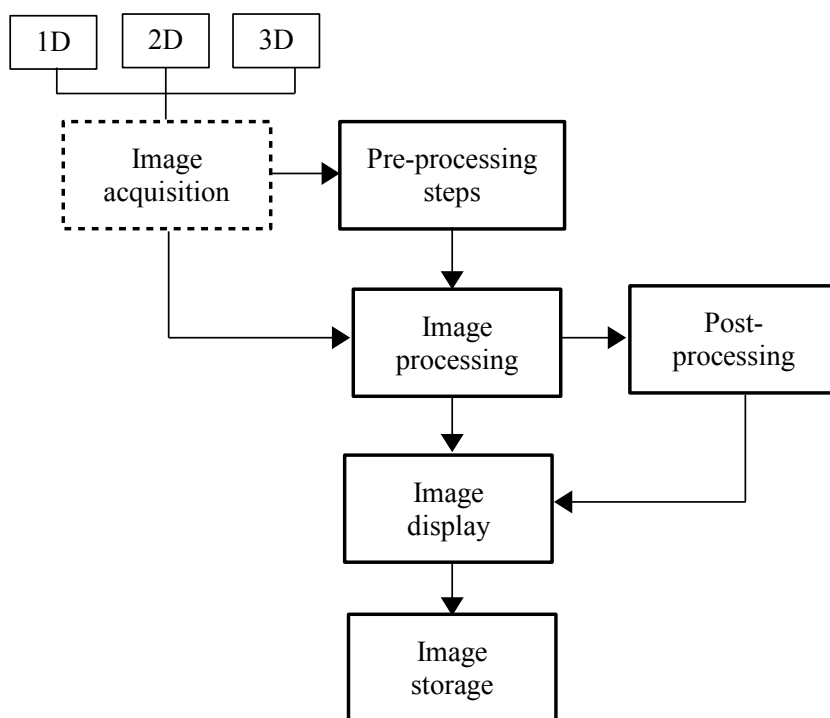
Figure 1.1: The image processing components, emphasizes on the focus of the study

2

1.1.1 Imaging modalities
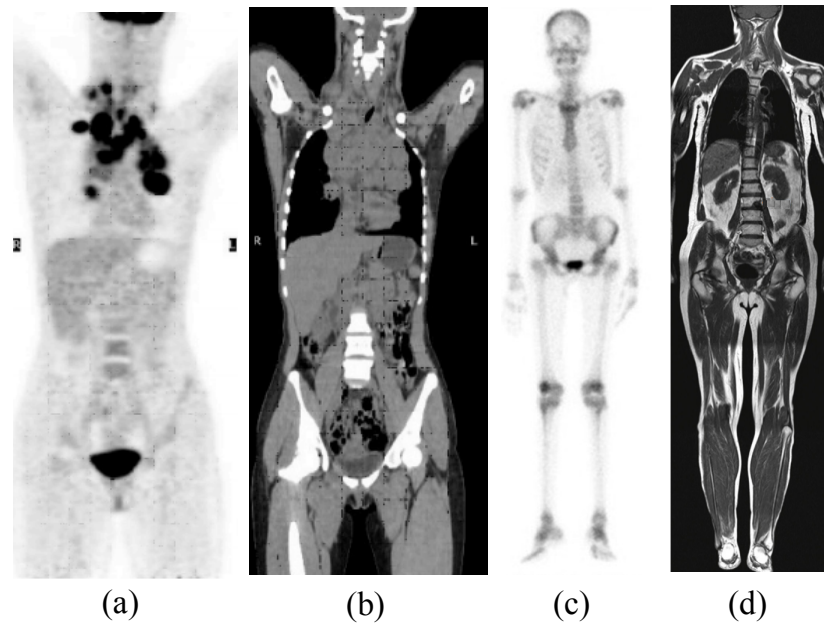
Figure 1.2: Examples of whole body images acquired using various imaging modalities (a) PET [19] (b) CT [19] (c) SPECT [20] (d) MRI [21]

Currently, many medical imaging modalities are available in the market. Some of the modalities are invented for the specific aims of usage. For instance, mammography is specifically invented for the breast imaging and magnetic resonance imaging (MRI) for bones, joints and soft tissue imaging. Figure 1.2 shows examples of the whole body images acquired using different imaging modalities [19–21].

In general, each modality has advantages and disadvantages over the others. The attachment of the PET radioisotope with the glucose analog material (which is fluorodeoxyglucose, FDG) makes sensitivity of PET imaging in detecting the onset of a tumor superior to the other medical and nuclear imaging modalities. Ability of PET to detect the molecular changes offers earlier detection of cancer compares to the CT and MRI diagnosis which rely on the anatomical changes of the patient's body [22]. It is worth noting that the physical or anatomical changes in the patient's body, usually could be observed after a time frame following the onset of a disease. This characteristic makes PET imaging as the best modality for diagnosis, monitoring and staging of cancer [9, 10]. It is well known that the relationship between photon sensitivity and spatial resolution in medical imaging is always reciprocal [23, 24]. Thus, a good sensitivity PET scanner will have a trade-off of its spatial resolution. Yet, this disadvantage had been resolved by the introduction of the dual modality imaging, for instance, PET/CT and PET/MRI [25].

The other nuclear imaging modality available in clinical practices is the gamma camera. The camera works by detecting single gamma photon emitted from the patient's body. It differs from the PET imaging in the sense that the photon emitter's radioisotope is used.

In comparison to the PET scanner, gamma camera has a lower sensitivity and spatial resolution [26]. The big slab of Sodium Iodide (NaI) scintillation detector in gamma camera limits the spatial resolution of this modality. Fortunately, there is a study on a new collimator called wire mesh collimator that could increase both the sensitivity and spatial resolution of a gamma camera [27]. In addition, there is also a hybrid imaging technique that incorporates SPECT and CT in a gantry [28]. Other than that, the SPECT radioisotopes are cheaper compared to the PET radioisotopes. They also have a longer half-life, i.e. several hours to days compares to several minutes to hours for PET radioisotopes. Availability of on-site generators at a reasonable cost for SPECT radioisotopes also gives another additional advantage of SPECT over PET. However, for a whole-body imaging, SPECT imaging requires longer acquisition time and may cause the patient to feel uncomfortable.

Aside from nuclear imaging modalities, there are other imaging modalities like X-ray, mammography, fluoroscopy and CT scanner. Being different from the nuclear imaging modalities, these modalities work by X-ray transmission from the target material to the patient's body. While conventional X-ray is restricted to the static image acquisition, fluoroscopy offers advantages in dynamic studies. The CT scanner is the best choice to be considered when imaging the structure based, like the bone and blood vessels. Some of the imaging modalities for medical purposes are invented based on the usage of the non-ionizing radiation, for instance, MRI and ultrasound. This radiation, which has less energy than the ionizing radiation is thus less risky to the patient. In summary, each modality might give advantages over the others depending on the purpose of usage. The summary on the characteristics of each imaging technique is listed in Table 1.1 and Table 1.2.

4

Table 1.1: Comparison of the imaging techniques

Imaging technique		Main characteristics	Applications	Advantages	Disadvantages
PET		• Coincidence event detection • Positron emitter radioisotope	• Metabolic • Functional • Molecular	• Higher sensitivity than SPECT • Higher spatial resolution than SPECT (~4 to 6 mm)[26]	• High cost cyclotron • Shorter half-life radioisotopes compares to SPECT
SPECT		• Single photon detection • Gamma emitter radioisotope	• Functional	• Longer half-life radioisotope than PET • Lower cost, on site radioisotope generator	• Less sensitivity than PET • Less spatial resolution (~15 mm)[26]
CT		• Collimated source and detector • Contrast agent for image contrast enhancement	• Anatomical • Functional	• Commonly used for structural based imaging, like bone • Higher resolution than nuclear imaging	• Poor soft tissue contrast • High radiation dose

Table 1.2: Comparison of the imaging techniques (continue)

Imaging technique	Main characteristics	Applications	Advantages	Disadvantages
MRI	• Electromagnet and radio frequency pulses	• Anatomical • Functional • Molecular	• Best for soft tissue contrast than other techniques • Higher resolution than nuclear imaging • Radiation dose free	• Expensive procedure • Limited to metallic devices free patient
Ultrasound	• High frequency sound wave application • Microbubbles needed for contrast enhancement	• Anatomical • Functional	• Detail of soft tissue images • Non-invasive • Radiation dose free	• Limited image resolution • Poor visualization for bone • Image quality and interpretation is personal dependence

1.1.2 PET Imaging
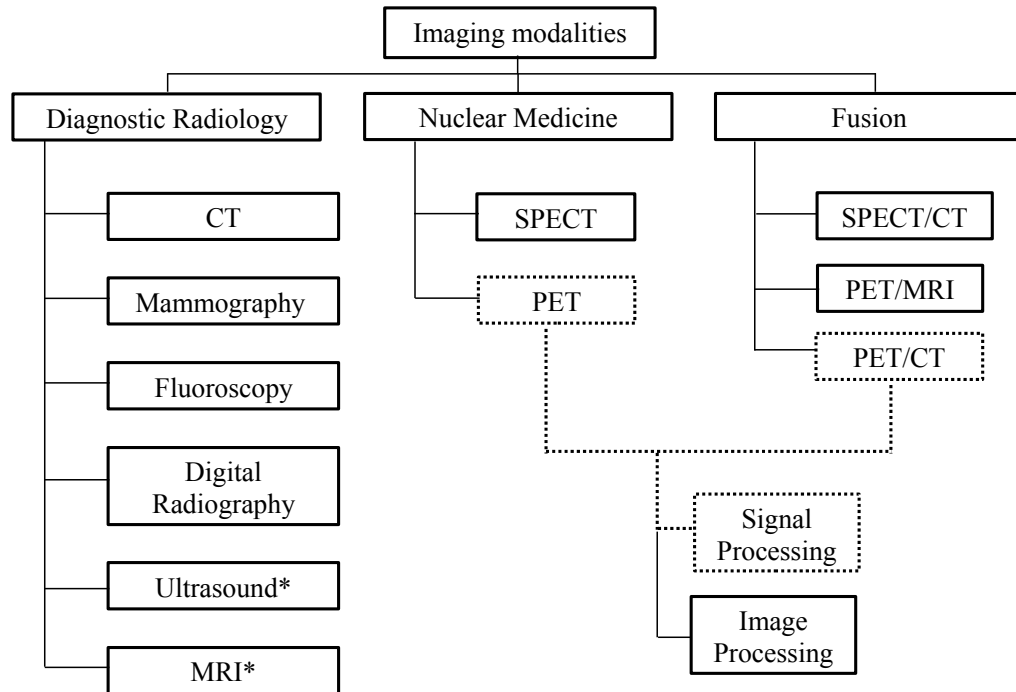
* refer to imaging modalities that utilize the application of non-ionizing radiation.

Figure 1.3: Summary of the imaging modalities used for diagnostic purpose and the direction focused in this study

As discussed in the previous section, varieties of imaging modalities have been developed with the purpose of medical diagnosis and monitoring. Generally, these modalities could be classified into two categories, namely diagnostic radiology and nuclear medicine imaging modalities. In addition to that, a fusion technology that incorporates both diagnostic radiology and nuclear medicine modalities in a single gantry is available. The classification of these imaging modalities is summarized in the flow chart shown in Figure 1.3.

Current technology does offer combination of both diagnostic radiology and nuclear imaging modalities in a single scanner, for instance, PET/CT, SPECT/CT, PET/MRI and SPECT/MR [29]. In addition to that, multimodality or commonly called as hybrid imaging modality has become a research interest nowadays. The examples of other hybrid system are the Opti-SPECT/PET/CT, PET/SPECT/CT and PET/optical imaging [30–34]. Most of these hybrid systems are still in the stage of pre-clinical trial and laboratory research. Of all existing imaging equipment, this study focuses on the signal processing of the PET scanner. Figure 1.4 shows the image of the Siemens Biograph TruePoint PET/CT scanner modeled in this study. Optimization of the signal, i.e. in the sense of the energy window that restricts the extension of PET data to be counted for image reconstruction is the focus of this study.

Figure 1.4: Siemens Biograph TruePoint PET/CT scanner used as a reference in this study

PET imaging works based on the detection of coincidence photons that are emitted at approximately 180° each other. The radioisotopes for PET imaging are positron emitters, for instance Fluorine-18 (^{18}F), Oxygen-15 (^{15}O), Carbon-11 (^{11}C) and Nitrogen-13 (^{13}N). The maximum positron energy (and half-life) of each are 635 keV (110 min), 1720 keV (2.07 min), 970 keV (20.4 min) and 1190 keV (9.96 min). Following the injection of the radioisotope into the patient's bloodstream, the material is distributed throughout the patient's body. Basically, this material follows the glucose pathway, as it is tagged with the FDG. Interestingly, the active cells like tumor, brain and heart consume more glucose than the normal cell due to the high metabolic activity of the cells. Thus, the tumor cell, which absorbs more radiotracer appears brighter compares to the normal cell in the reconstructed image. The tumor appearance with respect to the normal cell in the reconstructed image is termed as the hot spots.

1.2   Problem Statement

Compton scatter is one of the predominant interactions within the patient's body. This interaction causes a high number of scatter events detected in PET imaging. The photon interaction cross-section for a wide range of photon energy is illustrated in Figure 1.5 [1]. For the lower atomic number of the material, the probability of Compton interaction covers a relatively broad area. The Compton effect dominates within the energy range of 20 keV to 30 MeV at the respective lower atomic number material. The human body, which highly contributes by the lower atomic number of materials, thus causes the Compton interaction to dominate. For instance, the effective atomic number of bone and soft tissue is 11.6-13.8 and 7.4 respectively [35]. In addition to that, the probability of scatter interaction increases with the increment of the patient's body weight. This situation is encountered when imaging of an overweight or obese patient. Imaging of a relatively big patient causes the image to be contributed by a higher fraction of scattered

8

data and thus noisy [36]. The method proposed in this study is therefore aimed to minimize the contribution of scatter events in PET imaging, especially for the higher density human body.

The examples of methods are currently practiced to reject the scattered photon include the use of septa in 2D acquisition, scatter correction and the energy threshold level setting [18, 37, 38]. The energy threshold level that is commonly manipulated to reject the scattered photons is the lower energy threshold level. Theoretically, a PET scanner will have a perfect energy resolution by accepting only 511 keV photons. Unfortunately, this method is impractical to be implemented in the real life situation. A longer acquisition time is required to acquire statistically enough photons for image reconstruction if such finite energy resolution is practiced. In addition to that, more counts could be gained by injection of higher radioactivity and better efficiency of a scanner. Inadequate number of counts during image reconstruction causes the image to be influenced by the artifact [39]. Indeed, a relatively long acquisition time will lead to other disadvantages, for instance, patient motion artifacts and patient inconvenience [9, 40]. Therefore, the energy threshold level for PET imaging usually sets to cover some range of energy and called as the lower and upper energy threshold level. The energy threshold level of a scanner usually specified by the vendor may vary depending on the configurations of the scanner, particularly the type of the detector material [12, 41].
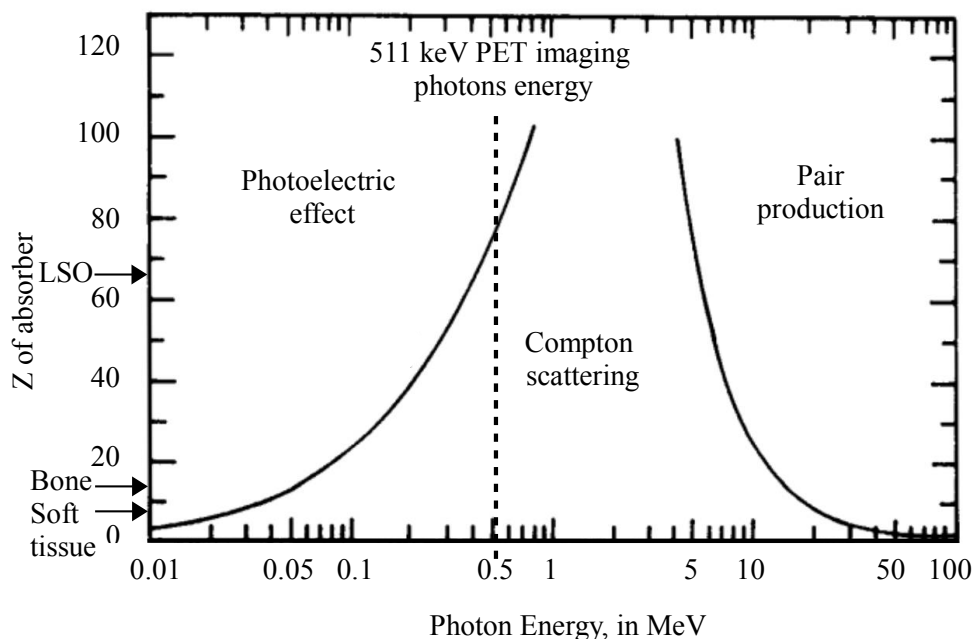
Figure 1.5: The photon interaction cross-section, presented for the various photon energy and effective atomic number of the medium. Adapted from [1]

9

Surveys of the literature reveal that the most commonly used energy threshold level for the clinical LSO-based PET scanner is in the range of 300 keV to 425 keV for lower energy threshold level and 590 keV to 665 keV (with the most common practise is 650 keV) for upper energy threshold level [12, 41–44]. Those levels usually set at a constant setting for a particular PET study. One of the problems with this is when dealing with different sizes of the patient's body. The different sizes of the patient's body (some previously studied by different sizes of phantom) lead to a different fraction of scattered and attenuated event counted in the PET data [18, 39, 40, 45–47]. Therefore, based on the data of phantom study, PET image acquisition using a constant level of energy threshold for different sizes of the patient's body could overestimate or underestimate the scatter fraction [18, 47]. Our effort was therefore to determine the optimal energy threshold level for the different sizes of a patient's body. This target was achieved based on the simulation of various sizes of human-shaped phantom using Monte Carlo N-particle (MCNP) code version MCNP5.

In conclusion to all the explanations previously discussed, the factors that contribute to the onset idea of this research are as below:

1. The natural characteristic of human body, which comprises of low atomic number materials leads to high probability of scatter interactions at the respective energy range involves in PET imaging [1, 35].

2. The probability of the scatter interaction and photon attenuation increases with the increment of the weight of the patient [40, 46]. Thus, imaging of a bigger size patient would lead to noisier PET image compares to the smaller patient [36].

3. Current practices in our institution, which apply a constant energy window and constant dose, would cause the overestimation or underestimation of the scatter fraction when the various sizes of patient's imaging are considered [18, 47].

1.3 Aim and Objectives

The aim of this study is to determine the optimum value of energy threshold level for LSO-based PET scanner, focusing for different sizes of human-shaped phantom which represent the underweight, normal, overweight and obese patients. To achieve the aim, we therefore set the following specific objectives:

1. To model the PET scanner using Monte Carlo code version MCNP5 and validate experimentally with Siemens Biograph TruePoint PET/CT.

2. To investigate and relate the effect of human body mass to the scatter fraction and visibility of a tumor.

3. To determine and formulate the optimal energy threshold level for the different sizes of phantom.

1.4 Scope and Limitation of the Study
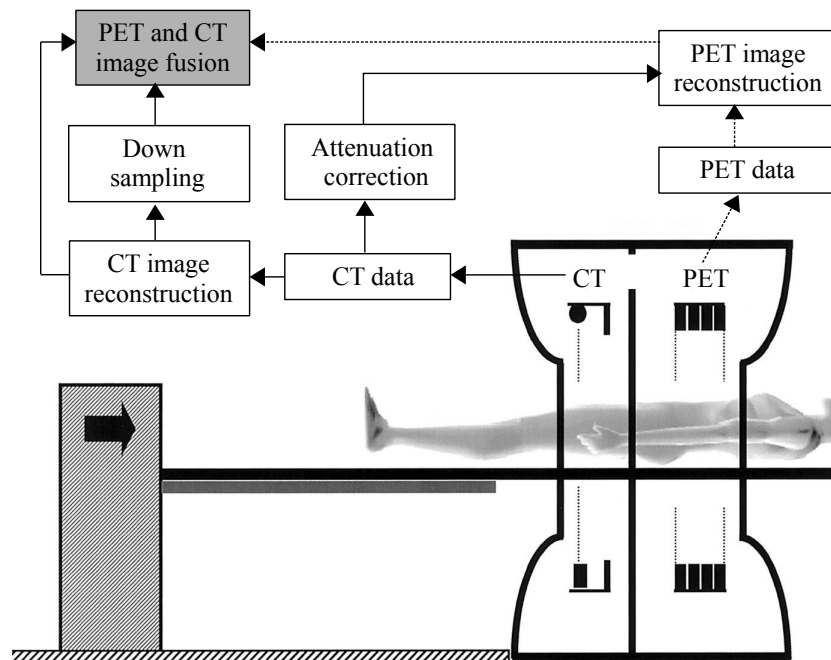
Figure 1.6: The data flow in PET/CT scanner. Each PET and CT data are treated individually and are fused together at the end of the processing steps. Adapted from [48]

This study focuses on the definition of the optimal energy threshold level for LSO-based PET imaging based on a validated MCNP5 code. Initially, we developed the PET scanner MCNP5 code based on the technical specification of Siemens Biograph TruePoint PET/CT. The dual modalities offer by this hybrid scanner interestingly enables both PET and CT data to be processed individually (as shown in Figure 1.6) [48]. Hence, a hybrid scanner will provide us with three types of data or images. These data are PET image, CT image and PET/CT image. This characteristic enables us to focus on the PET data only. The improvement in the PET section thus will let similar improvement when PET/CT scanner is used. Therefore, the findings yielded from this study are applicable for both PET or PET/CT system. Development of a realistic PET scanner by using MCNP5 code is one of the important aspects of this study. Validation on the particular PET scanner modeled was conducted and presented in this study. The processes of our PET MCNP5 code verification was done via the comparison between simulated and experimental data.

In addition to the development of a realistic PET MCNP5 code, the other most important scope of this study is the different sizes of the phantom imaging modeled. Various phantom sizes were considered in this study to represent the different groups of a patient's body. Patient weights of 44.0 kg, 68.7 kg, 86.2 kg and 99.0 kg are approximated by four different sizes of elliptical-shape cylindrical phantoms. Estimation of the weight and eventually the body mass index (BMI) of the phantom were made

11

based on assumption of 175 cm height patient and pure water density [49]. The size of the normal phantom and eventually phantom's volume is comparable to the calibrated phantom which is the commercially available PET phantom. The phantoms, that are in the range of 20 cm to 30 cm major diameter are represented the underweight, normal, overweight and obese adult patients. The phantom volume, which was filled with water of 1 gcm^{-3} density, thus approximates the photon interactions within the human body.

The next discussion is to explain the validity of the data obtained in this study, of which a water-filled phantom was modeled to represent the different BMI patients. The relationship between weight gains, increases in waist circumference and evenly total body fat have been discussed by a previous study [50]. Compton scattering, that is the dominant interaction within the photon energy range involves in PET imaging is dependent on electron per unit volume. Therefore, this interaction is affected by the electron density and physical density of the material encountered by the photon. The differences between the electron density of bone, fat, muscle and water are not more than 10% because it is proportional to the atomic number to atomic mass ratio [51]. In addition to that, the electron density of approximately similar for both of the materials also documented. Fat and water have an electron density of 3.34 to $3.48x10^{26}$ and $3.34x10^{26}$ each [35]. It should be noted that the Compton scattering is not affected by the atomic number of the material as it involves the loosely bound electron. The effective atomic numbers of 5.9 to 6.3 and 7.4 have been reported for fat and water respectively [35]. As a conclusion, Compton scattering is thus assumed to be affected by the physical density of the material only.

A photon might be attenuated either through absorption or scattering when pass through a material. This characteristic is described by the linear attenuation coefficient or the mass attenuation coefficient. Nevertheless, the attenuation rate is commonly expressed in terms of the mass of the medium that is passed through by the photon namely mass attenuation coefficient [3, 52]. Referring to Figure 1.7, the mass attenuation coefficient of fat and soft tissue are not significantly varied at photon energy of 100 keV and greater [53]. Therefore, the probability of fat and water (which modeled to approximate the soft tissue interaction) to be attenuated either by the absorption or Compton scattering is not significantly varied at the photon's energy involved in PET imaging. Based on this argument, we believe that this water-filled phantom is representing the scattering behavior within the different BMI of a patient's body.
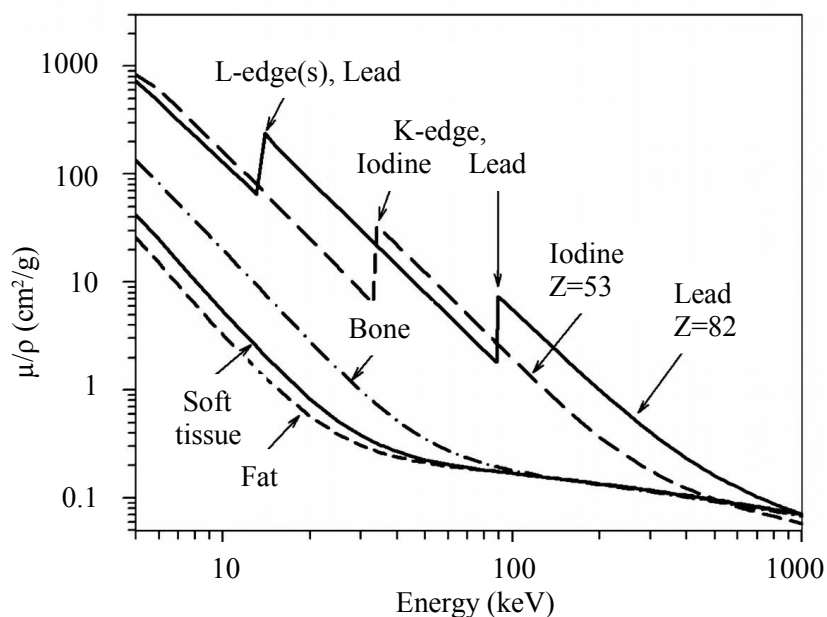
Figure 1.7: The mass attenuation coefficient for the various materials involved in imaging presented for as a function of photon energy. Adapted from [53].

The simulations of the various phantom imaging used similar initial random seed number. The model thus randomly sampling the similar behavior of the photon emitted from the various phantoms. Each simulation model was then repeated using three different initial random seed numbers to observe the standard error of the data. Decrement in the statistical uncertainty of the data as the number of photon history modeled increases had been declared by previous study [54].

In PET imaging, there are three types of data that let to coincidence events registration. Those data are true coincidence, scatter coincidence and random coincidence. The latter two data are those that contributed to the noise in the reconstructed image. In this study, we did not model the random coincidence due to absence of real timeliness of interaction information in the simulation output. The absence of random noise modeling after all is expected to not significantly affect the characteristic of the parameters tested in this study. The random event, which is unrelated to the patient's body weight, is affected by the activity present [36, 41]. A constant average random fraction at approximately 35% was reported in previous study for the relatively constant dose protocol implemented, when the various weights of patient's body imaging were performed [36]. The similar study also declared that the true coincidence lost with the increment of the patient's body weight is the reason for the degradation in the PET image quality for this imaging protocol. Therefore, the constant dose protocol concerns in this study is expected not to give significant variation in the random fraction when the various phantoms' imaging are performed. The noise that is solely contributed from the scatter interaction was therefore modeled in this study.

13

1.5 Contribution of the Thesis

The significant contribution of this thesis is in the optimal energy threshold level definition for the underweight, normal and obesity patients. The definitions of the energy threshold levels were made based on phantoms modeling using a validated MCNP5 code. The current energy threshold level practices commonly did not vary among the different sizes of the patient's body. Indeed, the fraction of scatter interactions within the patient's body is affected by the size or weight of the patient's body. Therefore, implementation of the optimal energy threshold level for each size of phantom is necessary to minimize the contribution of noise in the reconstructed PET image. In addition to that, the other significant contribution of this study is on the derivation of an equation that correlates among the body weight, TBR or SUV of the tumor and the optimal energy threshold level. This equation is therefore much valuables in definition of the optimal energy window for the specific imaging conditions. Other than that, we also managed to develop as realistic as possible model of a PET scanner using MCNP5 code. Development of this PET scanner code is much useful in understanding the physical principles of photon interactions in PET imaging. Further study associated with the PET imaging is therefore possible and applicable by using this simulation code. We have also submitted the data obtained in this study to be published in several related journals, and even presented at several international conferences.

The main contributions of the study can be summarized into three:

1. Development of a guideline on the optimal energy threshold level for the underweight, normal and obesity patients to be used in PET or PET/CT scanner.

2. Derivation of equations on the optimal energy threshold level calculation, with full consideration on the patient's body weight and TBR as well as SUV of the tumor.

3. Development of a realistic PET MCNP5 simulation code for PET scanner modeling which can be used as a testbed.

REFERENCES

[1] F. H. Attix, *Introduction to radiological physics and radiation dosimetry*. USA: A Wiley-Interscience Publication, 1986.

[2] K. Iniewski, *Medical Imaging: Principles, Detectors, and Electronics*. Hoboken, New Jersey: John Wiley & Sons, 2009.

[3] J. Bushberg, J. Seibert, E. Leidholdt, and J. Boone, *The Essential Physics of Medical Imaging*. USA: Lippincott Williams and Wilkins, 2011.

[4] P. E. Valk, D. Delbeke, D. L. Bailey, D. W. Townsend, and M. N. Maisey, *Positron Emission Tomography: Clinical Practice*. London: Springer Science & Business Media, 2006.

[5] K. Kubota, "From tumor biology to clinical PET: a review of positron emission tomography (PET) in oncology," *Annual Nuclear Medicine*, vol. 15, no. 6, pp. 471–486, 2001.

[6] O. Couturier, A. Luxen, J. F. Chatal, J. P. Vuillez, P. Rigo, and R. Hustinx, "Fluorinated tracers for imaging cancer with positron emission tomography," *European Journal of Nuclear Medicine and Molecular Imaging*, vol. 31, no. 8, pp. 1182–1206, 2004.

[7] G. C. C. Lim, S. Rampal, and Y. Halimah, "The Third Report of the National Cancer Registry: Cancer incidence in Peninsular Malaysia, 2003 - 2005," *National Cancer Registry*, 2008.

[8] O. Z. Ariffin and I. T. N. Saleha, "National Cancer Registry Report: Peninsular Malaysia cancer statistics - data and figure 2006," *Malaysia: National Cancer Registry, Ministry of Health*, 2006.

[9] B. S. Halpern, M. Dahlbom, A. Quon, C. Schiepers, C. Waldherr, D. H. Silverman, O. Ratib, and J. Czernin, "Impact of patient weight and emission scan duration on PET/CT image quality and lesion detectability," *Journal of Nuclear Medicine*, vol. 45, no. 5, pp. 797–801, 2004.

[10] R. Boellaard, M. J. ODoherty, W. A. Weber, F. M. Mottaghy, M. N. Lonsdale, S. G. Stroobants, and et al., "FDG PET and PET/CT: EANM procedure guidelines for tumour PET imaging: version 1.0," *European Journal of Nuclear Medicine and Molecular Imaging*, vol. 37, no. 1, pp. 181–200, 2010.

[11] K. Fiedler, T. Frach, W. Rutten, T. Solf, and A. Thon, "Assessment of the spatial resolution of PET scanners using a Geant4-based Monte Carlo Tool," in *IEEE Nuclear Science Symposium Conference Record*, vol. 4, 2004, pp. 2549–2553.

[12] G. Tarantola, F. Zito, and P. Gerundini, "PET instrumentation and reconstruction algorithms in whole-body application," *Journal of Nuclear Medicine*, vol. 44, no. 5, pp. 756–769, 2003.

[13] K. Shibuya, E. Yoshida, T. Nishikido, T. Suzuki, T. Tsuda, N. Inadama, T. Yamaya, and H. Muruyama, "Limit of spatial resolution in FDG-PET due to annihilation photon non-collinearity," in *World Congress on Medical Physics and Biomedical Engineering 2006 IFMBE Proceedings*, vol. 14, 2007, pp. 1667–1671.

[14] H. Murayama, "Recent advances in PET and the new jPET-D4 system," in *World Congress on Medical Physics and Biomedical Engineering 2006 IFMBE Proceedings*, vol. 14, 2007, pp. 1684–1687.

[15] M. E. Daube-Witherspoon, J. S. Karp, M. E. Casey, F. P. DiFilippo, H. Hines, G. Muehllehner, V. Simcic, C. W. Stearns, L. E. Adam, S. Kohlmyer, and V. Sossi, "PET performance measurements using the NEMA NU 2-2001 standard," *Journal of Nuclear Medicine*, vol. 43, no. 10, pp. 1398–1409, 2002.

[16] H. Herzog, L. Tellmann, C. Hocke, U. Pietrzyk, M. E. Casey, and T. Kuwert, "NEMA NU2-2001 guided performance evaluation of four Siemens ECAT PET scanners," *IEEE Transactions on Nuclear Science*, vol. 51, no. 5, pp. 2662–2669, 2004.

[17] C. Riddell, R. E. Carson, J. A. Carrasquillo, S. K. Libutti, D. N. Danforth, M. Whatley, and S. L. Bacharach, "Noise reduction in oncology FDG PET images by iterative reconstruction: a quantitative assessment," *Journal of Nuclear Medicine*, vol. 42, no. 9, pp. 1316–1323, 2001.

[18] A. Konik, M. Madsen, and J. Sunderland, "GATE simulations of human and small animal PET for determination of scatter fraction as a function of object size," *IEEE Transactions on Nuclear Science*, vol. 57, no. 5, pp. 2558–2563, 2010.

[19] M. Pagano, M. Berta, A. M. Postini, M. Bianchi, A. B. del Prever, C. Defillippi, U. Ficola, and A. Cistaro, "Nonossifying fibroma: A possible pitfall in F18-FDG-PET/CT imaging of Hodgkin's disease," *Radiology Case Reports*, vol. 6, no. 2, pp. 1–4, 2011.

[20] S. Nilegaonkar, R. Karekar, D. Hirawe, and S. Lagade, "Adult onset Still's disease: Role of scintigraphy," *Indian Journal of Nuclear Medicine*, vol. 27, no. 1, pp. 48–49, 2012.

[21] F. E. Lecouvet, J. E. Mouedden, L. Collette, E. Coche, E. Danse, F. Jamar, J. Machiels, B. V. Berg, P. Omoumi, and B. Tombal, "Can whole-body magnetic resonance imaging with diffusion-weighted imaging replace Tc 99m bone scanning and computed tomography for single-step detection of metastases in patients with high-risk prostate cancer?" *European Urology*, vol. 62, no. 1, pp. 68–75, 2012.

[22] V. Kapoor, B. M. McCook, and F. S. Torok, "An introduction to PET-CT imaging," *Radiographics*, vol. 24, no. 2, pp. 523–543, 2004.

[23] A. Rahmim and H. Zaidi, "PET versus SPECT: strengths, limitations and challenges," *Nuclear Medicine Communications*, vol. 29, no. 3, pp. 193–207, 2008.

[24] L. R. MacDonald, W. C. J. Hunter, P. E. Kinahan, and R. S. Miyaoka, "Effects of detector thickness on geometric sensitivity and event positioning errors in the rectangular PET/X scanner," *IEEE Transactions on Nuclear Science*, vol. 60, no. 5, pp. 3242–3252, 2013.

[25] M. R. Ay and S. Sarkar, "Computed tomography based attenuation correction in PET/CT: principles, instrumentation, protocols, artifacts and future trends," *Iranian Journal of Nuclear Medicine*, vol. 15, no. 2, pp. 1–29, 2007.

[26] D. L. Bailey and K. P. Willowson, "An evidence-based review of quantitative SPECT imaging and potential clinical applications," *Journal of Nuclear Medicine*, vol. 54, pp. 83–89, 2013.

[27] W. H. M. Saad, R. E. Roslan, M. A. Mahdi, C. W. Seng, E. Saion, and M. I. Saripan, "Monte Carlo design of optimal wire mesh collimator for breast tumor imaging process," *Nuclear Instruments and Methods in Physics Research, Section A: Accelerators, Spectrometers, Detectors and Associated Equipment*, vol. 648, no. 1, pp. 254–260, 2011.

[28] A. K. Buck, S. Nekolla, S. Ziegler, A. Beer, B. J. Krause, K. Herrmann, K. Scheidhauer, H. Wester, E. J. Rummeny, M. Schwaiger, and A. Drzezga, "SPECT/CT," *Journal of Nuclear Medicine*, vol. 49, pp. 1305–1319, 2008.

[29] S. R. Cherry, "Multimodality imaging: Beyond PET/CT and SPECT/CT," *Seminars in Nuclear Medicine*, vol. 39, no. 5, pp. 348–353, 2009.

[30] C. Li, Y. Yang, G. S. Mitchell, and S. R. Cherry, "Simultaneous PET and multispectral 3-dimensional fluorescence optical tomography imaging system for small animals," *Journal of Nuclear Medicine*, vol. 52, pp. 1268–1275, 2011.

[31] N. T. Vu, R. W. Silverman, and A. F. Chatziioannou, "Preliminary performance of optical PET (OPET) detectors for the detection of visible light photons," *Nuclear Instruments and Methods in Physics Research, Section A: Accelerators, Spectrometers, Detectors and Associated Equipment*, vol. 569, no. 2, pp. 563–566, 2006.

[32] Society of Nuclear Medicine, "Opti-SPECT/PET/CT: five different imaging systems now combined," www.sciencedaily.com, June Retrieved 03/12/2014.

[33] J. Culver, W. Akers, and S. Achilefu, "Multimodality molecular imaging with combined optical and SPECT/PET modalities," *Journal of Nuclear Medicine*, vol. 49, no. 2, pp. 169–172, 2008.

[34] TriFoil Imaging, "Triumph II PET/SPECT/CT imaging: total solution for preclinical tri-modality (PET/SPECT/CT) in-vivo imaging," http://www.trifoilimaging.com, Retrieved 03/12/2014.

[35] W. R. Hendee and E. R. Ritenour, *Medical Imaging Physics, Fourth Edition*. USA: Wiley-Liss, Inc, 2002.

[36] A. Nagaki, M. Onoguchi, and N. Matsutomo, "Patient weight-based acquisition protocols to optimize ^{18}F-FDG PET/CT image quality," *Journal of Nuclear Medicine Technology*, vol. 39, no. 2, pp. 72–76, 2011.

[37] T. G. Turkington, J. W. Wilson, and J. G. Colsher, "Adjusting the low energy threshold for large bodies in PET," in *IEEE Nuclear Science Symposium Conference Record*, vol. 5, 2004, pp. 2872–2876.

[38] M. Lubberink, A. van Schie, H. W. A. M. de Jong, G. A. M. S. van Dongen, and G. J. J. Teule, "Acquisition setting for PET of ^{124}I administered simultaneously with therapeutic amounts of ^{131}I," *Journal of Nuclear Medicine*, vol. 47, no. 8, pp. 1375–1381, 2006.

[39] T. G. Turkington, "Introduction to PET instrumentation," *Journal of Nuclear Medicine Technology*, vol. 29, no. 1, pp. 4–11, 2001.

[40] B. S. Halpern, M. Dahlbom, M. A. Auerbach, C. Schiepers, B. J. Fueger, W. A. Weber, D. H. Silverman, O. Ratib, and J. Czernin, "Optimizing imaging protocols for overweight and obese patients: a lutetium orthosilicate PET/CT study," *Journal of Nuclear Medicine*, vol. 46, no. 4, pp. 603–607, 2005.

[41] P. Zanzonico, "Positron emission tomography: a review of basic principles, scanner design and performance and current systems," *Seminars in Nuclear Medicine*, vol. 34, no. 2, pp. 87–111, 2004.

[42] Y. E. Erdi, S. A. Nehmeh, T. Mulnix, J. L. Humm, and C. C. Watson, "PET performance measurements for an LSO-based combined PET/CT scanner using the National Electrical Manufacturers Association NU 2-2001 standard," *Journal of Nuclear Medicine*, vol. 45, no. 5, pp. 813–821, 2004.

[43] M. Brambilla, C. Secco, M. Dominietto, R. Matheoud, G. Sacchetti, and E. Inglese, "Performance characteristics obtained for a new 3-dimensional lutetium oxyorthosilicate-based whole-body PET/CT scanner with the National Electrical Manufacturers Association NU 2-2001 standard," *Journal of Nuclear Medicine*, vol. 46, no. 12, pp. 2083–2091, 2005.

[44] T. Carlier, T. Eugene, C. Bodet-Milin, E. Garin, C. Ansquer, C. Rousseau, L. Ferrer, J. Barbet, F. Schoenahl, and F. Kraeber-Bodere, "Assessment of acquisition protocols for routine imaging of Y-90 using PET/CT," *EJNMMI Research*, vol. 3, no. 11, pp. 1–12, 2013.

[45] S. Vallabhajosula, *Molecular Imaging: Radiopharmaceuticals for PET and SPECT*. New York: Springer Science and Business Media, 2009.

[46] G. E. Fakhri, P. A. Santos, R. D. Badawi, C. H. Holdsworth, A. D. V. D. Abbeele, and M. F. Kijewski, "Impact of acquisition geometry, image processing, and patient size on lesion detection in whole-body 18F-FDG PET," *Journal of Nuclear Medicine*, vol. 48, no. 12, pp. 1951–1960, 2007.

[47] A. Ferrero, J. K. Poon, A. J. Chaudhari, L. R. MacDonald, and R. D. Badawi, "Effect of object size on scatter fraction estimation methods for PET- a computer simulation study," *IEEE Transactions on Nuclear Science*, vol. 58, no. 1, pp. 82–86, 2011.

[48] H. Zaidi, "Optimisation of whole-body PET/CT scanning protocols," *Biomedical Imaging and Intervention Journal*, vol. 3, no. 2, pp. 1–9, 2007.

[49] E. H. de Groot, N. Post, R. Boellaard, N. R. L. Wagenaar, A. T. M. Willemsen, and J. A. van Dalen, "Optimized dose regimen for whole-body FDG-PET imaging," *EJNMMI Research*, vol. 3, no. 63, pp. 1–11, 2013.

[50] J. P. Despres, "Body fat distribution and risk of cardiovascular disease: an update," *Circulation*, vol. 126, pp. 1301–1313, 2010.

[51] P. Allisy-Roberts and J. R. Williams, *Farr's physics for medical imaging*. Europe: Elsevier Health Sciences, 2007.

[52] P. Sprawls, *Physical Principles of Medical Imaging*. USA: Aspen Publisher, 1987.

[53] J. A. Seibert and J. M. Boone, "X-ray imaging physics for nuclear medicine technologists. Part 2: X-ray interactions and image formation," *Journal of Nuclear Medicine Technology*, vol. 33, pp. 3–18, 2005.

[54] N. D. Mukhopadhyay, A. J. Sampson, D. Deniz, G. A. Carlsson, J. Williamson, and A. Malusek, "Estimating statistical uncertainty of Monte Carlo efficiency-gain in the context of a correlated sampling Monte Carlo code for brachytherapy treatment planning with non-normal dose distribution," *Applied Radiation and Isotopes*, vol. 70, no. 1, pp. 315–323, 2012.

[55] A. Ohtani, K. Tanaka, T. Mizuta, Y. Inoue, H. Tonami, J. Ohi, and K. Kitamura, "Optimization of enhanced energy window on a whole-body DOI PET system," in *IEEE Nuclear Science Symposium Conference Record*, 2009, pp. 3618–3621.

[56] A. R. Yu, J. S. Kim, K. M. Kim, Y. S. Lee, S. K. Woo, W. H. Lee, J. G. Kim, J. I. Park, H. J. Kim, and G. J. Cheon, "Optimal PET acquisition setting of I-124 with Siemens Inveon PET: comparative simulation study with F-18 and microPET R4," in *IEEE Nuclear Science Symposium Conference Record*, 2009, pp. 2666–2668.

[57] N. Karakatsanis and K. Nikita, "A simulation model of the counting-rate response of clinical PET systems and it's application to optimize the injected dose," in *IEEE International Symposium on Biomedical Imaging*, 2009, pp. 398–401.

[58] C. Lartizien, C. Comtat, P. E. Kinahan, N. Ferreira, B. Bendriem, and R. Trebossen, "Optimization of injected dose based on noise equivalent count rates for 2- and 3-dimensional whole-body PET," *Journal of Nuclear Medicine*, vol. 43, no. 9, pp. 1268–1278, 2002.

[59] L. Brunsveld, *Supramolecular Systems in Biomedical Fields*. USA: ChemBioChem, 2014.

[60] C. Lois, B. W. Jakoby, M. J. Long, K. F. Hubner, D. W. Barker, M. E. Casey, M. Conti, V. Y. Panin, D. J. Kadrmas, and D. Townsend, "An assessment of the impact of incorporating time-of-flight information into clinical PET/CT imaging," *Journal of Nuclear Medicine*, vol. 51, no. 2, pp. 237–245, 2010.

[61] M. Conti, "Effect of randoms on signal-to-noise ratio in TOF PET," *IEEE Transactions on Nuclear Science*, vol. 53, no. 3, pp. 1188–1193, 2006.

[62] M. Phelps, *PET: Physics, instruments, and scanners*, ser. VI. USA: Springer, 2006.

[63] C. L. Melcher, "Scintillation crystals for PET," *Journal of Nuclear Medicine*, vol. 41, pp. 1051–1055, 2000.

[64] S. Tavernier, *Experimental Techniques in Nuclear and Particle Physics*. London: Springer, 2010.

[65] S. A. Dyer, *Wiley Survey of Instrumentation and Measurement*. London: John Wiley & Sons, 2004.

[66] Hamamatsu Photonics, "PMT (photomultiplier tubes)," http://www.hamamatsu.com, Retrieved 17/12/2014.

[67] W. Qingyang, W. Shi, M. Tianyu, M. Fei, D. Tiantian, X. Tianpeng, W. Zhaoxia, J. Yongjie, and L. Yaqiang, "Influence factors of two dimensional position map on photomultiplier detector block designed by quadrant sharing technique," *Nuclear Science and Techniques*, vol. 22, no. 4, pp. 224–229, 2011.

[68] B. J. Pichler, B. K. Swann, J. Rochelle, R. E. Nutt, S. R. Cherry, and S. B. Siegel, "Lutetium oxyorthosilicate block detector readout by avalanche photodiode arrays for high resolution animal PET," *Physics in Medicine and Biology*, vol. 49, no. 18, pp. 4305–4319, 2004.

[69] J. Kang, Y. Choi, K. J. Hong, W. Hu, J. Y. Hwang, H. K. Lim, Y. Huh, S. Kim, K. B. Kim, J. W. Jung, Y. H. Chung, and B.-T. Kim, "PET detector configuration with thick light guide and GAPD array having large-area microcells," in *IEEE Nuclear Science Symposium Conference Record*, 2010, pp. 2495–2499.

[70] D. Dowsett and P. Kenny, *The Physics of Diagnostic Imaging, Second Edition*. London: Hodder Arnold, 2010.

[71] W. Qingyang, Y. Liu, M. Tianyu, X. Yan, W. Shi, W. Zhaoxia, and J. Yongjie, "PMT-cross-display scintillator block detector design and Monte Carlo study," in *IEEE Nuclear Science Symposium Conference Record*, 2010, pp. 2400–2402.

[72] S. Ahmed, *Physics and Engineering of Radiation Detection*. USA: Academic Press, 2007.

[73] M. Wernick and J. Aarsvold, *Emission Tomography: The Fundamentals of PET and SPECT*. USA: Academic Press, 2004.

[74] O. Mawlawi, J. W. Wilson, T. Pan, and T. G. Turkington, "Investigating the optimum lower energy threshold of a new research PET/CT scanner," in *IEEE Nuclear Science Symposium Conference Record*, vol. 4, 2005, pp. 2054–2056.

[75] I. Castiglioni, O. Cremonesi, M. C. Gilardi, A. Savi, V. Bettinardi, G. Rizzo, E. Bellotti, and F. Fazio, "A Monte Carlo model of noise components in 3D PET," *IEEE Transactions on Nuclear Science*, vol. 49, no. 5, pp. 2297–2303, 2002.

[76] E. Yoshida, K. Kitamura, F. Nishikido, K. Shibuya, T. Hasegawa, T. Yamaya, N. Inadama, and H. Murayama, "Feasibility study of a highly sensitive LaBr$_3$ PET scanner based on the DOI-dependent extended-energy window," *Nuclear Instruments and Methods in Physics Research Section A: Accelerators, Spectrometers, Detectors and Associated Equipment*, vol. 604, no. 1-2, pp. 363–365, 2009.

[77] E. Yoshida, K. Kitamura, K. Shibuya, F. Nishikido, T. Hasegawa, T. Yamaya, and H. Murayama, "A DOI-dependent extended energy window method to control balance of scatter and true events," in *IEEE Nuclear Science Symposium Conference Record*, vol. 4, 2007, pp. 2611–2616.

[78] F. H. Fahey, "Data acquisition in PET imaging," *Journal of Nuclear Medicine Technology*, vol. 30, no. 2, pp. 39–49, 2002.

[79] I. Polycarpou, P. K. Marsden, and C. Tsoumpas, "A comparative investigation of scatter correction in 3D PET ," *Journal of Physics: Conference Series*, vol. 317, pp. 1–4, 2011.

[80] P. E. Kinahan, B. H. Hasegawa, and T. Beyer, "X-ray-based attenuation correction for positron emission tomography/computed tomography scanners," *Seminars in Nuclear Medicine*, vol. 33, no. 3, pp. 166–179, 2003.

[81] IAEA, *IAEA Human Health Series No. 27. PET/CT Atlas on Quality Control and Image Artefacts*, ser. 1. Vienna International Centre, PO Box 100, 1400 Vienna, Austria: IAEA, 2014.

[82] D. Bailey, D. Townsend, P. Valk, and M. Maisey, *Positron Emission Tomography: Basic sciences*. London: Springer-Verlag, 2005.

[83] D. Brasse, P. E. Kinahan, C. Lartizien, C. Comtat, M. Casey, and C. Michel, "Correction methods for random coincidences in fully 3D whole-body PET: impact on data and image quality," *Journal of Nuclear Medicine*, vol. 46, no. 5, pp. 859–867, 2005.

[84] B. Bai, Q. Li, C. H. Holdsworth, E. Asma, Y. C. Tai, A. Chatziioannou, and R. M. Leahy, "Model-based normalization for iterative 3D PET image reconstruction," *Physics in Medicine and Biology*, vol. 47, no. 15, pp. 2773–2784, 2002.

[85] M. L. Camborde, A. Rhamim, D. F. Newport, S. Siegel, K. R. Buckley, E. Vandervoort, T. J. Ruth, and V. Sossi, "Effect of normalization method on image uniformity and binding potential estimates on microPET," in *IEEE Nuclear Science Symposium Conference Record*, vol. 6, 2004, pp. 3467–3471.

[86] R. D. Badawi and P. K. Marsden, "Developments in component-based normalization for 3D PET," *Physics in Medicine and Biology*, vol. 44, no. 2, pp. 571–594, 1999.

[87] E. Vicente, J. J. Vaquero, S. Espana, J. L. Herraiz, J. M. Udias, and M. Desco, "Normalization in 3D PET: Dependence on the activity distribution of the source," in *IEEE Nuclear Science Symposuim Conference Record*. IEEE, pp. 2206–2209.

[88] T. Oakes, V. Sossi, and T. Ruth, "Normalization in 3D PET: comparison of detector efficiencies obtained from uniform planar and cylindrical sources," in *IEEE Nuclear Science Symposium Conference Record*, vol. 2, 1997, pp. 1625–1629.

[89] G. B. Saha, *Basics of PET Imaging*. New York, NY: Springer New York, 2010.

[90] J. P. J. Carney and D. W. Townsend, "Clinical count rate performance of an LSO PET/CT scanner utilizing a new front-end electronics architecture with sub-nanosecond intrinsic timing resolution," *Radiation Physics and Chemistry*, vol. 75, no. 12, pp. 2182–2185, 2006.

[91] L. Eriksson, D. Townsend, M. Conti, M. S. M. Eriksson, H. Rothfuss, M. E. Casey, and B. Bendriem, "An investigation of sensitivity limits in PET scanners," *Nuclear Instruments and Methods in Physics Research, Section A: Accelerators, Spectrometers, Detectors and Associated Equipment*, vol. 580, no. 2, pp. 836–842, 2007.

[92] S. R. Cherry, J. A. Sorenson, and M. E. Phelps, *Physics in Nuclear Medicine*. Saunders (W.B.) Co Ltd., 2003.

[93] B. W. Jakoby, Y. Bercier, C. C. Watson, B. Bendriem, and D. W. Townsend, "Performance characteristics of a new LSO PET/CT scanner with extended axial field-of-view and PSF reconstruction," *IEEE Transactions on Nuclear Science*, vol. 56, no. 3, pp. 633–639, 2009.

[94] J.-C. Cheng, S. Blinder, A. Rahmim, and V. Sossi, "A scatter calibration technique for dynamic brain imaging in high resolution PET," *IEEE Transactions on Nuclear Science*, vol. 57, no. 1, pp. 225–233, 2010.

[95] H. Zaidi, *Quantitative Analysis in Nuclear Medicine Imaging*. USA: Springer Science & Business Media, 2006.

[96] Sureshbabu, Waheeda, and O. Mawlawi, "PET/CT imaging artifacts," *Journal of Nuclear Medicine Technology*, vol. 33, no. 3, pp. 156–61, 2005.

[97] P. E. Kinahan, D. W. Townsend, T. Beyer, and D. Sashin, "Attenuation correction for a combined 3D PET/CT scanner," *Medical Physics*, vol. 25, no. 10, pp. 2046–2053, 1998.

[98] A. Alessio and P. Kinahan, *PET image reconstruction, In: Nuclear Medicine (2nd ed.)*. Philadelphia: Elsevier, 2006.

[99] M. Lyra and A. Ploussi, "Filtering in SPECT image reconstruction," *International Journal of Biomedical Imaging*, vol. 2011, pp. 1–14, 2011.

[100] A. L. Goertzen, Q. Bao, M. Bergeron, E. Blankemeyer, S. Blinder, M. Caadas, A. F. Chatziioannou, K. Dinelle, E. Elhami, H. S. Jans, E. Lage, R. Lecomte, V. Sossi, S. Surti, Y. C. Tai, J. J. Vaquero, E. Vicente, D. A. Williams, and R. Laforest, "NEMA NU 4-2008 comparison of preclinical PET imaging systems," *Journal of Nuclear Medicine*, vol. 53, no. 8, pp. 1300–1309, 2012.

[101] H. K. Son, M. J. Yun, T. J. Jeon, D. O. Kim, H. J. Jung, J. D. Lee, H. S. Yoo, and H. J. Kim, "ROC analysis of ordered subset expectation maximization and filtered back projection technique for FDG-PET in lung cancer," *Nuclear Science Symposium Conference Record*, vol. 3, pp. 1801–1805, 2001.

[102] C. J. Jaskowiak, J. A. Bianco, S. B. Perlman, and J. P. Fine, "Influence of reconstruction iterations on 18F-FDG PET/CT standardized uptake values," *Journal of Nuclear Medicine*, vol. 46, no. 3, pp. 424–428, 2005.

[103] H. Schoder, Y. E. Erdi, K. Chao, M. Gonen, S. M. Larson, and W. D. Yeung, "Clinical implications of different image reconstruction parameters for interpretation of whole-body PET studies in cancer patients," *Journal of Nuclear Medicine*, vol. 45, no. 4, pp. 559–566, 2004.

[104] J. L. Herraiz, S. Espana, J. M. Udias, J. J. Vaquero, and M. Desco, "Statistical reconstruction methods in PET: resolution limit, noise, edge artifacts and considerations for the design of better scanners," in *IEEE Nuclear Science Symposium Conference Record*, 2005, pp. 1846–1850.

150

[105] A. Sanchez-Crespo, P. Andreo, and S. A. Larsson, "Positron flight in human tissues and its influence on PET image spatial resolution," *European Journal of Nuclear Medicine and Molecular Imaging*, vol. 31, no. 1, pp. 44–51, 2004.

[106] G. J. Kemerink, M. G. Visser, R. Franssen, E. Beijer, M. Zamburlini, S. G. Halders, B. Brans, F. M. Mottaghy, and G. J. Teule, "Effect of the positron range of 18F, 68Ga and 124I on PET/CT in lung-equivalent materials," *European Journal of Nuclear Medicine and Molecular Imaging*, vol. 38, no. 5, pp. 940–948, 2011.

[107] A. Sanchez-Crespo and S. A. Larsson, "The influence of photon depth of interaction and non-collinear spread of annihilation photons on PET image spatial resolution," *European Journal of Nuclear Medicine and Molecular Imaging*, vol. 33, no. 8, pp. 940–947, 2006.

[108] H. Zaidi, *Molecular Imaging of Small Animals: Instrumentation and Applications*. New York: Springer Science & Business Media, 2014.

[109] IAEA, *IAEA Human Health Series No. 1. Quality Assurance For PET and PET/CT Sytems*, ser. 1. Vienna International Centre, PO Box 100, 1400 Vienna, Austria: IAEA, 2009.

[110] J. Cal-Gonzalez, J. L. Herraiz, S. Espana, M. Desco, J. J. Vaquero, and J. M. Udias, "Positron range effects in high resolution 3D PET imaging," in *IEEE Nuclear Science Symposium Conference Record*, 2009, pp. 2788–2791.

[111] D. W. Townsend, "Physical principles and technology of clinical PET imaging," *Annals of the Academy of Medicine*, vol. 33, no. 2, pp. 133–145, 2004.

[112] B. McIntosh, D. B. Stout, and A. L. Goertzen, "Validation of a GATE model of 176 Lu intrinsic radioactivity in LSO PET systems," *IEEE Transactions on Nuclear Science*, vol. 58, no. 3, pp. 682 – 686, 2011.

[113] S. Lashkari, S. Sarkar, M. R. Ay, and A. Rahmim, "The influence of crystal material on intercrystal scattering and the parallax effect in PET block detectors: a Monte Carlo study," *Iranian Journal of Medical Physics*, vol. 21, pp. 67–76, 2008.

[114] P. P. Bruyant, J. Sau, and J. Mallet, "Streak artifact reduction in filtered backprojection using a level line-based interpolation method," *Journal of Nuclear Medicine*, vol. 41, no. 11, pp. 1913–1919, 2000.

[115] S. Tong, A. M. Alessio, K. Thielemans, C. Stearns, S. Ross, and P. E. Kinahan, "Properties of edge artifacts in reconstruction PSF-based PET reconstruction," in *IEEE Nuclear Science Symposuim Conference Record*. IEEE, 2010, pp. 3649–3652.

[116] W. Moses, "Time of flight in PET revisited," *IEEE Transactions on Nuclear Science*, vol. 50, no. 5, pp. 1325–1330, 2003.

[117] Y. Masuda, C. Kondo, Y. Matsuo, M. Uetani, and K. Kusakabe, "Comparison of imaging protocols for 18F-FDG PET/CT in overweight patients: optimizing scan duration versus administered dose," *Journal of Nuclear Medicine*, vol. 50, no. 6, pp. 844–848, 2009.

[118] N. Efthimiou, G. Loudos, N. A. Karakatsanis, and G. Panayotakis, "^{176}Lu effect on the minimum detectable activity limits for a dual head, LSO:Ce based, PET system," in *Nuclear Science Symposium Conference Record*, 2013, pp. 1–3.

[119] D. C. Vines, H. Keller, J. D. Hoisak, and S. L. Breen, "Quantitative PET comparing gated with nongated acquisitions using a NEMA phantom with respiratory-simulated motion," *Journal of Nuclear Medicine Technology*, vol. 35, no. 4, pp. 246–251, 2007.

[120] A. M. Alessio, M. Sammer, G. S. Phillips, V. Manchanda, B. C. Mohr, and M. T. Parisi, "Evaluation of optimal acquisition duration or injected activity for pediatric 18F-FDG PET/CT," *Journal of Nuclear Medicine*, vol. 52, no. 7, pp. 1028–1034, 2011.

[121] A. M. J. Paans, G. Rosenqvist, S. Holte, L. Eriksson, M. Dahlbom, and C. Bohm, "Scatter fraction: measurement and correction," *European Journal of Nuclear Medicine*, vol. 15, no. 11, pp. 727–731, 1989.

[122] J. P. J. Carney, J. T. Yap, and D. W. Townsend, "PET count rate performance and CT image quality of a 16-slice LSO PET/CT for clinical whole-body imaging," *Radiation Physics and Chemistry*, vol. 71, no. 3-4, pp. 963–965, 2004.

[123] R. Accorsi, J. S. Karp, and S. Surti, "Improved dose regimen in pediatric PET," *Journal of Nuclear Medicine*, vol. 51, no. 2, pp. 293–300, 2010.

[124] H. Everaert, C. Vanhove, T. Lahoutte, K. Muylle, V. Caveliers, A. Bossuyt, and P. R. Franken, "Optimal dose of 18F-FDG required for whole-body PET using an LSO PET camera," *European Journal of Nuclear Medicine and Molecular Imaging*, vol. 30, no. 12, pp. 1615–1619, 2003.

[125] M. Tatsumi, P. A. Clark, Y. Nakamoto, and R. L. Wahl, "Impact of body habitus on quantitative and qualitative image quality in whole-body FDG-PET," *European Journal of Nuclear Medicine and Molecular Imaging*, vol. 30, no. 1, pp. 40–45, 2003.

[126] D. J. Kadrmas, M. E. Casey, M. Conti, B. W. Jakoby, C. Lois, and D. W. Townsend, "Impact of time-of-flight on PET tumor detection," *Journal of Nuclear Medicine*, vol. 50, no. 8, pp. 1315–1323, 2009.

[127] A. Kuhn, S. Surti, J. S. Karp, P. S. Raby, K. S. Shah, A. E. Perkins, and G. Muehllehner, "Design of a lanthanum bromide detector for time-of-flight PET," *IEEE Transactions on Nuclear Science*, vol. 51, no. 5, pp. 2550–2557, 2004.

[128] D. W. Rogers, "Fifty years of Monte Carlo simulations for medical physics," *Physics in Medicine and Biology*, vol. 51, no. 13, pp. R287–301, 2006.

[129] C. Lartizien, A. Reilhac, N. Costes, M. Janier, and D. Sappey-Marinier, "Monte Carlo simulation-based design study of a LSO-LuAP small animal PET system," *IEEE Transactions on Nuclear Science*, vol. 50, no. 5, pp. 1433–1438, 2003.

[130] C. Groiselle, Y. D'Asseler, J. A. Kolthammer, C. G. Matthews, and S. J. Glick, "A Monte Carlo simulation study to evaluate septal spacing using triple-head hybrid PET imaging," *IEEE transactions on Nuclear Science*, vol. 50, no. 5, pp. 1339–1346, 2003.

[131] F. Lamare, M. J. L. Carbayo, G. Kontaxakis, A. Santos, A. Turzo, Y. Bizais, C. Cheze Le Rest, and D. Visvikis, "Incorporation of elastic transformations in list-mode based reconstruction for respiratory motion correction in PET," in *IEEE Nuclear Science Conference Record*, vol. 3, 2005, pp. 1740–1744.

[132] S. Staelens, Y. D'Asseler, S. Vandenberghe, M. Koole, I. Lemahieu, and R. V. de Walle, "A three-dimensional theoretical model incorporating spatial detection uncertainty in continuous detector PET," *Physics in Medicine and Biology*, vol. 49, no. 8, pp. 2337–2351, 2004.

[133] B. Guérin and G. E. Fakhri, "Realistic PET Monte Carlo simulation with pixelated block detectors, light sharing, random coincidences and dead-time modeling," *IEEE transactions on Nuclear Science*, vol. 55, no. 3, pp. 942–952, 2008.

[134] L. L. Meunier, F. Mathy, and D. Fagret, "Validation of a PET monte-carlo simulator with random events and dead time modeling," *IEEE Transactions on Nuclear Science*, vol. 50, no. 5, pp. 1462–1468, 2003.

[135] D. Nikolopoulos, S. Kottou, N. Chatzisavvas, X. Argyriou, E. Vlamakis, P. Yannakopoulos, and A. Louizi, "A GATE simulation study of the Siemens Biograph DUO PET/CT system," *Open Journal of Radiology*, vol. 3, no. 2, pp. 56–65, 2013.

[136] S. Jan, C. Comtat, D. Strul, G. Santin, and R. Trebossen, "Monte Carlo simulation for the ECAT EXACT HR+ system using GATE," *IEEE Transactions on Nuclear Science*, vol. 52, no. 3, pp. 627–633, 2005.

[137] S. Jan, J. Collot, M. Gallin-Martel, P. Martin, F. Mayet, and E. Tournefier, "GePEToS : A Geant4 Monte Carlo simulation package for Positron Emission Tomography," *IEEE Transactions on Nuclear Science*, vol. 52, no. 1, pp. 102–106, 2005.

[138] S. Espana, J. L. Herraiz, E. Vicente, J. J. Vaquero, M. Desco, and J. M. Udias, "PeneloPET, a Monte Carlo PET simulation tool based on PENELOPE: features and validation," *Physics Medicine and Biology*, vol. 54, no. 6, pp. 1723–1742, 2009.

[139] C. J. Thompson, J. Moreno-Cantu, and Y. Picard, "PETSIM: Monte Carlo simulation of all sensitivity and resolution parameters of cylindrical positron imaging systems," *Physics in Medicine and Biology*, vol. 37, no. 3, pp. 731–749, 1992.

[140] M. I. Saripan, M. Petrou, and K. Wells, "Design of a wire-mesh collimator for gamma cameras," *IEEE Transactions on Biomedical Engineering*, vol. 54, no. 9, pp. 1598–1612, 2007.

153

[141] M. I. Saripan, W. H. M. Saad, S. Hashim, R. Mahmud, A. J. Nordin, and M. A. Mahdi, "Monte carlo simulation on breast cancer detection using wire mesh collimator gamma camera," *IEEE Transactions on Nuclear Science*, vol. 56, no. 3, pp. 1321–1324, 2009.

[142] R. E. Roslan, W. H. M. Saad, M. I. Saripan, S. Hashim, and W. S. Choong, "The performance of a wire mesh collimator SPECT camera for different breast volumes in prone position," *Nuclear Instruments and Methods in Physics Research, Section A: Accelerators, Spectrometers, Detectors and Associated Equipment*, vol. 619, no. 1-3, pp. 385–387, 2010.

[143] J. Lantos, S. Czifrus, D. Legrady, and A. Cserkaszky, "Detector response function of the NanoPET^{TM}/CT system," in *Nuclear Science Symposium Conference Record*, 2010, pp. 3641–3643.

[144] J. Lantos, S. Czifrus, G. Patay, and T. Bukki, "MCPS - an MCNPX based simulation tool for modeling the physical behavior of PET systems," *IEEE Transactions on Nuclear Science*, vol. 61, no. 1, pp. 134 – 141, 2014.

[145] I. Kambali, T. Heryanto, Rajiman, and S. Ichwan, "Reliability study of the liquid target chamber for ^{18}F production at the BATANs cyclotron facilities ," *Atom Indonesia*, vol. 37, no. 1, pp. 5–10, 2011.

[146] IAEA, *IAEA Technical Report Series No. 465 Cyclotron Produced Radionuclides: Principles and Practice*, ser. 465. Vienna International Centre, PO Box 100, 1400 Vienna, Austria: IAEA, 2008.

[147] A. M. Paans, A. van Waarde, P. H. Elsinga, A. T. Willemsen, and W. Vaalburg, "Positron emission tomography: the conceptual idea using a multidisciplinary approach," *Methods*, vol. 27, no. 3, pp. 195–207, 2002.

[148] A. Priyanka, S. K. Rathi, and A. S. Verma, "Continuous slowing down approximation (CS and DA) ranges of electrons and positrons for Carbon, Aluminium and Copper," *Research Journal of Recent Sciences*, vol. 1, no. 6, pp. 70–76, 2012.

[149] MedWOW Ltd. Global, "Manufacturer specifications-Siemens Biograph64 TruePoint PET/CT," http://www.medwow.com/med/petct/siemens/biograph-64-truepoint-petct/34158.model-spec, Retrieved 31/12/2014.

[150] P. Cheebsumon, R. Boellaard, D. de Ruysscher, W. van Elmpt, A. van Baardwijk, M. Yaqub, O. S. Hoekstra, E. F. I. Comans, A. A. Lammertsma, and F. H. P. van Velden, "Assessment of tumour size in PET/CT lung cancerstudies: PET- and CT-based methods compared to pathology," *EJNMMI Research*, vol. 2, no. 56, pp. 1–9, 2012.

[151] F. Aydin, L. Dertsiz, E. S. Budak, A. Yildiz, G. Ozbilim, and F. Gungor, "Measurements of tumor size using CT and PET compared to histopathological size in non-small cell lung cancer," *Diagnostic and Interventional Radiology*, vol. 19, no. 4, pp. 271–278, 2013.

[152] D. J. de Vries, S. C. Moore, R. E. Zimmerman, S. P. Mueller, B. Friedland, and R. C. Lanza, "Development and validation of a Monte Carlo simulation of photon transport in an Anger camera," *IEEE Transactions on Medical Imaging*, vol. 9, no. 4, pp. 430–438, 1990.

[153] G. Nelson and D. Reilly, *Passive Nondestructive Analysis of Nuclear Materials*. Los Alamos National Laboratory,, 1991.

[154] M. Charron, *Pediatric PET Imaging*. New York, USA: Springer Science & Business Media, 2006.

[155] M. Conti, I. Hong, and C. Michel, "Reconstruction of scattered and unscattered PET coincidences using TOF and energy information," *Physics in Medicine and Biology*, vol. 57, no. 15, pp. N307–N317, 2012.

[156] C. C. Watson, M. E. Casey, L. Eriksson, T. Mulnix, D. Adams, and B. Bendriem, "NEMA NU 2 performance tests for scanners with intrinsic radioactivity," *Journal of Nuclear Medicine*, vol. 45, no. 5, pp. 822–826, 2004.

[157] *MCNP: A General Monte Carlo N-Particle Transport Code Version 5*. X-5 Monte Carlo Team, 2003.

[158] C. H. Holdsworth, C. S. Levin, T. H. Farquhar, M. Dahlbom, and E. J. Hoffman, "Investigation of accelerated Monte Carlo techniques for PET simulation and 3D PET scatter correction," *IEEE Transactions on Nuclear Science*, vol. 48, no. 1, pp. 74–81, 2001.

[159] A. K. Mansoor and K. R. Indra, "Pharmaceutical and Clinical Calculations," 2000.

[160] Biodex Medical Systems, "PET phantoms," http://www.biodex.com, Retrieved 07/11/2014.

[161] ARGH Industries Ltd, "How to convert volume to weight," http://www.thecalculatorsite.com, Retrieved 07/11/2014.

[162] N. Ibrahim, F. M. Moy, I. A. N. Awalludin, Z. Ali, and I. S. Ismail, "The health-related quality of life among pre-diabetics and its association with body mass index and physical activity in a semi-urban community in Malaysia- a cross sectional study," *BMC Public Health*, vol. 14, no. 298, pp. 1–10, 2014.

[163] C. S. Levin, A. M. K. Foudray, and F. Habte, "Impact of high energy resolution detectors on the performance of a PET system dedicated to breast cancer imaging," *Physica Medica*, vol. 21, no. 1, pp. 28–34, 2006.

[164] M. Soret, S. L. Bacharach, and I. Buvat, "Partial-volume effect in PET tumor imaging," *Journal of Nuclear Medicine*, vol. 48, no. 6, pp. 932–945, 2007.

[165] I. V. Khodyuk, J. T. M. de Haas, and P. Dorenbos, "Non-proportional response between 0.1-100keV energy by means of highly monochromatic synchrotron X-rays," *IEEE Transactions on Nuclear Science*, vol. 57, no. 3, pp. 1175–1181, 2011.

[166] Department of Physics and Astronomy, George State University, "X-rays transitions," http://hyperphysics.phy-astr.gsu.edu, Retrieved 07/11/2014.

[167] S. A. Nehmeh, H. El-Zeftawy, C. Greco, J. Schwartz, Y. E. Erdi, A. Kirov, C. R. Schmidtlein, A. B. Gyau, S. M. Larson, and J. L. Humm, "An iterative technique to segment PET lesions using a Monte Carlo based mathematical model," *Medical Physics*, vol. 36, no. 10, pp. 4803–4809, 2009.

[168] M. Khalil, *Basic Sciences of Nuclear Medicine*. Springer Science & Business Media, 2010.

[169] R. K. Doot, J. S. Scheuermann, P. E. Christian, J. S. Karp, and P. E. Kinahan, "Instrumentation factors affecting variance and bias of quantifying tracer uptake with PET/CT," *Medical Physics*, vol. 37, no. 11, pp. 6035–6046, 2010.